Water Management in PEMFC

D.S. Falcão[1], C.M. Rangel[2] , C.Pinho[1], A.M.F.R. Pinto[1]

[1]Centro de Estudos de Fenómenos de Transporte, Faculdade de Engenharia da Universidade do Porto, Portugal
email:apinto@fe.up.pt
[2]Instituto Nacional de Engenharia, Tecnologia e Inovação, Portugal
email: carmen.rangel@ineti.pt

Abstract

The potential of fuel cells for clean and efficient energy conversion is generally recognized. Proton-exchange membrane (PEM) Fuel Cells are among the different types of fuel cells one of the most promising. The water management is a critical problem to overcome in the PEM fuel cell technology. Despite several studies on this topic effective water management is still elusive. Models play an important role in fuel cell development since they enable the understanding of the influence of different parameters on the cell performance allowing a systematic simulation, design and optimization of fuel cells systems.
In this work, a model previously developed and validated [1], is used to predict the water transport through the cell. The model takes into account heat and mass transport effects The influence of membrane thickness and transport properties, GDL thickness and structure, reactants pressure and humidification temperatures, on the water content through the membrane and on the cell performance was studied. All these parameters have an important impact in the cell water management. The model predicts the membrane water contents and water concentration profiles along the MEA. This work represents a useful tool to set-up suitable operating conditions and optimized tailored MEAs to produce a better performance of PEM fuel cells.

Keywords: *PEM fuel cell; heat and mass transfer, modeling, water management*

Nomenclature

a	Activity
A^s	Channels area (cm^2)
C	Concentration (mol/cm^3)
C*	Integration constant
D^{eff}	Effective diffusivity (cm^2/s)
D_λ^{eff}	Water membrane effective diffusivity (cm^2/s)
F	Faraday's constant (C/mol)
I_{cell}	Current density (A/cm^2)
i_0	Exchange current density (A/cm^2)
K	Partition Coefficient
L	Length (cm)
M_m	Membrane equivalent weight (kg/mol)
N	Molar flux ($mol/cm^2.s$)
$n_{channels}$	Number of channels
n_{drag}^{sat}	Electro-osmotic drag coefficient
P	Pressure (atm)
Q	Volumic flow (cm^3/s)
R	Universal gas constant (J/mol.K)
RH	Relative humidity (%)
R_m	Membrane electrical resistance ($\Omega.cm^2$)
T	Temperature (K)
V	Voltage (V)
W	Width (cm)
z	Coordinate (cm)

Greek letters

α	Net water transport coefficient
α_a	Anode transfer coefficient
α_c	Cathode transfer coefficient
γ^a	Anode concentration dependence
γ^c	Cathode concentration dependence
η	Overpotential (V)
λ	Membrane water content
ρ_{dry}	Dry membrane density (kg/cm^3)
ξ	Stoichiometry flow ratio

Subscripts

H_2	Hydrogen
H_2O	Water
in	Inlet
O_2	Oxygen
Sat	Saturation value

Superscripts

AACE	Acetate anode sheet
AAL	Anode aluminium plate
ABL	Anode backing layer
AC	Anode channel
ACL	Anode catalyst layer
ACu	Anode copper plate
AGraph	Anode graphite plate
CACE	Acetate cathode sheet
CAL	Cathode aluminium plate
CBL	Cathode backing layer

CC	Cathode channel
CCL	Cathode catalyst layer
CCu	Cathode copper plate
CGraph	Cathode graphite plate
in	Inlet
M	Membrane
Ref	Reference value

1 Introduction

Fuel cells are an innovative alternative to current power sources with potential to achieve higher efficiencies with renewable fuels with minimal environmental impact. In particular, the proton-exchange membrane (PEM) fuel cells are today in the focus of interest as one of the most promising developments in power generation with a wide range of applications in transportation and in portable electronics. Although prototypes of fuel cell vehicles and residential fuel cell systems have already been introduced, their cost must be reduced and their efficiencies enhanced.

Several coupled fluid flow, heat and mass transport processes occur in a fuel cell in conjunction with the electrochemical reactions. Generally, PEMFC operate bellow 80ºC. Anodic oxidation of hydrogen produces protons that are transported through the membrane to the cathode where the reduction of oxygen generates water. One of the most important operational issues of PEMFC is the water management in the cell [2, 3].

The water content of the membrane is determined by the balance between water production and three water transport processes: electro-osmotic drag of water (EOD), associated with proton migration through the membrane; back diffusion from the cathode to anode; and diffusion of water to/from the oxidant/fuel gas streams. Understanding the water transport in the PEM [4, 5] is a key issue to avoid cathode flooding and membrane dehydration and can also serve as a guide for materials optimization and development of new MEAs.

To improve the system performance, design optimization and analysis of fuel cell systems are important. Mathematical modelling and simulation are needed as tools for design optimization of fuel cells, stacks and fuel cells power systems.

Different models were developed in the last decade to describe several water transport mechanisms through the membrane such as Springer et al. [6] using a diffusion model, Bernardi and Verbrugge [7] considering a hydraulic permeation model and Kulikovsky [8] developing a semi analytical model 1D+1D taking into account oxygen and water transport across the cell and deriving an expression for the limiting current density.
To achieve optimal fuel cell performance, it is critical to have an adequate water balance to ensure that the membrane remains hydrated for sufficient proton conductivity while cathode flooding and anode dehydration are avoided [4,9,10].

In a previous work, Falcão et al [1] developed a semi-analytical one-dimensional model considering the effects of coupled heat and mass transfer, along with the electrochemical reactions occurring in PEMFC. The model can be used to predict the hydrogen, oxygen and water concentration profiles in the anode, cathode and membrane as well as the temperature profile across the cell. The model was validated with published experimental data.

The influence of the membrane thickness and transport properties, of the GDL thickness and structure, of the reactants pressure and humidification temperatures on the water content through the membrane and on the cell performance was simulated using the developed model.

2 Analytical Model

In the development of the model, the fuel cell is assumed as composed by different layers represented in Figure 1.

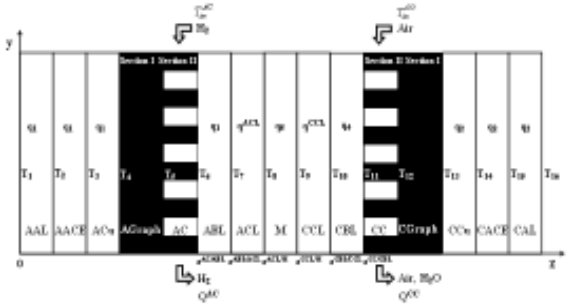

Figure 1. Schematic representation of a PEM fuel cell.

The cell consists in an aluminum plate (AL), an acetate sheet (ACE), a cupper current collector (Cu) and a flow channel (C), at the anode and cathode sides and a MEA. The MEA includes the backing layers (BL), the catalytic layers (CL) and the membrane (M). The acetate sheet isolates the end plate (aluminum), from the current collector plate.
At the anode side, the fuel H_2 (wet or humidified) is oxidized liberating electrons and producing protons while air (wet or humidified) is supplied to the cathode. The free electrons flow to the cathode, via an external circuit and there react with the protons and O_2, producing water and heat.
The model developed relies on the following assumptions:

- mass and heat transport are steady-state and one-dimensional (direction z in Figure 1);
- ideal gas mixture assumed;
- heat and mass transport through the gas diffusion and catalyst layers assumed to be a diffusion-predominated process (negligible convection effects);
- effective Fick models for the mass transport in the diffusion layers and membrane are considered;

- the thermal energy model is based on the differential thermal energy conservation equation (Fourier's law);
- the thermal conductivity for all the materials is assumed to be constant;
- the anodic and cathodic overpotential is constant through the catalyst layers;
- heat generation or consumption is considered in the catalyst layers;
- the heat generated by the current flow (Joule effects) through each cell layer is ignored;
- water transport through the membrane assumed to be a combined effect of diffusion and electro-osmotic drag;
- membrane proton conductivity is a function of λ, the number of water molecules per ionic group;
- local equilibrium at interfaces is represented by partition functions;
- reactions in the catalyst layers are considered as homogeneous;
- kinetics of the cathode is described by a Tafel expression;
- kinetics of the anode is described by a Tafel expression;
- anode and cathode flow channels are treated as a continuous stirred tank reactor (CSTR), so, the composition and temperature inside the channels are uniform;
- anode and cathode streams act as heat transfer fluids removing heat from the cell at the exit temperatures.

The development of the model is explained in detail in a previous work [1].

2.1 Water Balance

The values of water concentration at the catalytic layer (CL) were obtained considering mass transfer transport in the flow channels (C) and in backing layers (BL) along the z direction for both cathode and anode.

The flow channels are treated as a CSTR and the resulting equations are the following:

$$N_{H_2O}{}^{AC} = \alpha \frac{I_{cell}}{2F} = \frac{Q^{AC}}{A^s}\left(C_{H_2O}^{in} - C_{H_2O}^{AC/ABL}\right) \quad (1)$$

$$N_{H_2O}{}^{CC} = -(1+\alpha)\frac{I_{cell}}{2F} = \frac{Q^{CC}}{A^s}\left(C_{H_2O}^{in} - C_{H_2O}^{CC/CBL}\right) \quad (2)$$

where F is the Faraday constant, I_{cell} the cell current density and the net water transport coefficient, α, defined as:

$$\alpha = \frac{N_{H_2O}{}^{M}}{I_{cell}/2F} \quad (3)$$

In equations 1 – 2, the area A^s is given by:

$$A^s = n_{Channels} \times W \times L \quad (4)$$

where W and L are the channel width and length, respectively.

For the backing layers (BL) the transport equations are the following:

$$N_{H_2O}{}^{BL} = -D_{H_2O}^{eff,BL}\frac{dC_{H_2O}{}^{BL}}{dz} \quad (5)$$

where $D_{H_2O}^{eff,BL}$ is the water effective molecular diffusion coefficient through the backing layer.

For the catalytic layers (CL) the equations are:

$$N_{H_2O}{}^{CL} = -D_{H_2O}^{eff,CL}\frac{dC_{H_2O}{}^{CL}}{dz} \quad (6)$$

The species concentrations at the C/BL and BL/CL interfaces (for both cell sides) are giving by assuming local equilibrium with partition coefficients $K^{C/BL}$ and $K^{BL/CL}$ respectively. The boundary conditions for the set of equations (5) and (6) are:

$$\text{At } z = z^{C/BL} \rightarrow C_{H_2O}{}^{BL} = K^{C/BL}C^{C/BL} \quad (7)$$

$$\text{At } z = z^{BL/CL} \rightarrow C_{H_2O}{}^{CL} = K^{BL/CL}C^{BL/CL} \quad (8)$$

Using the set of differential equations (5) and (6) together with the boundary conditions (7) and (8), it is possible to determine the interface concentrations $C_{H_2O}^{ACL}$ and $C_{H_2O}^{CCL}$.

The water concentration at the anode and cathode catalyst layers, $C_{H_2O}^{ACL}$ and $C_{H_2O}^{CCL}$, is a function of the net water transport coefficient, α, (which, in turn, is a function of the membrane water content), and therefore α must be determined.

The water content in the membrane, λ, can be related with the water activity, a_{H_2O}, by O' Hayre et al.[11]:

$$\lambda = 14a_{H_2O} \text{ for } 0 < a_{H_2O} \le 1 \quad (9)$$

$$\lambda = 12.6 + 1.4a_{H_2O} \text{ for } 1 < a_{H_2O} \le 3 \quad (10)$$

The water activity can be defined as:

$$a_{H_2O} = \frac{C_{H_2O}RT}{P_{sat}} \quad (11)$$

where P_{sat} is the water saturation pressure at temperature T.

The water formation occurs at the cathode catalyst layer, therefore it was assumed that the water activity is less than 1 for the anode and higher than 1 for the cathode. Accordingly, to determine the water content at the interface ACL/membrane and at the interface CCL/membrane, one must use equations (9) and (10) respectively with the water activity calculated from equation (11). However, as the water activity is also a function of the water concentration, an alternative equation is necessary.

The water transport in the membrane can be described by considering electro-osmotic drag and back diffusion:

$$N_{H_2O}^{M} = 2n_{drag}^{sat}\frac{I_{cell}}{2F}\frac{\lambda}{22} - \frac{\rho_{dry}}{M_m}D_{\lambda}^{eff}(\lambda)\frac{\partial\lambda}{\partial z} \quad (12)$$

Where n_{drag}^{sat} is the electro-osmotic drag coefficient, D_{λ}^{eff} is the membrane water effective diffusivity, ρ_{dry} is the dry membrane density and M_m the membrane equivalent weight.

Substituting $N_{H_2O}^{M}$ by $\frac{\alpha I_{cell}}{2F}$ (from equation (3)) in equation (12) and integrating gives:

$$\lambda(z) = \frac{11}{n_{drag}^{sat}}\alpha + C^* \exp\left[\frac{I_{cell} M_m n_{drag}^{sat}}{22F\rho_{dry} D_{\lambda}^{eff}} z\right] \quad (13)$$

where C* is the integration constant.

For Nafion and Gore-Select membranes (types of membranes used in the simulations presented in this work) the effective water membrane diffusion coefficient is given by [12]:

$$D_{\lambda,Nafion}^{eff} = 10^{-6}\exp\left[2416\frac{1}{303} - \frac{1}{T}\right] \times\left(2.563 - 0.33\lambda + 0.0264\lambda^2 - 0.000671\lambda^3\right) \quad (14)$$

$$D_{\lambda,Gore-Select}^{eff} = 0.5\times\ D_{\lambda,Nafion}^{eff} \quad (15)$$

The values of the water content at the ACL/membrane and CCL/membrane interfaces are given by:

$$\lambda(z^{ACL/M}) = \frac{11}{n_{drag}^{sat}}\alpha + C^* \exp\left[\frac{I_{cell} M_m n_{drag}^{sat}}{22F\rho_{dry} D_{\lambda}^{eff}} z^{ACL/M}\right] \quad (16)$$

$$\lambda(z^{CCL/M}) = \frac{11}{n_{drag}^{sat}}\alpha + C^* \exp\left[\frac{I_{cell} M_m n_{drag}^{sat}}{22F\rho_{dry} D_{\lambda}^{eff}} z^{CCL/M}\right] \quad (17)$$

Using the set of differential equations (5) and (6) together with the boundary conditions (7) and (8), it is possible to determine the interface concentrations $C_{H_2O}^{ACL/M}$ and $C_{H_2O}^{CCL/M}$.

An iterative process is at this point set-up to determine the α parameter. Equaling equation (9) to equation (16) and equation (10) to equation (17) can be obtained the α parameter and the integration constant in function of membrane water diffusivity. Settling a value for membrane water diffusivity is possible to calculate water contents by equations (9) and (10) or (16) and (17). With water content value (an average value of anode and cathode water contents) is possible to calculate water membrane diffusivity by equations (14) or (15). At this point is used Solver from Excel and the process just stops when the difference between settling and calculated value of water membrane diffusivity is null, by changing the settling value.

All the model equations and the parameters values used to obtain the results presented in the next section can be found in a previous work [1].

3 Results and Discussion

The numerical tools used to implement the model were Matlab and Excel. The obtained predictions of the membrane water content and polarization curves after implementation of the model are presented. The basic set of conditions used to generate the simulations is summarized in table 1.

Table 1. Basic set of conditions used.

Cell Temperature (K)	298
Anode Flow Temperature (K)	298
Anode Relative Humidity (%)	50
Cathode Flow Temperature (K)	298
Cathode Relative Humidity (%)	50
Anode Pressure (atm)	1.2
Cathode Pressure (atm)	2
Anode Flow Rate (slpm)	0.23
Cathode Flow Rate (slpm)	0.33
Membrane active area (cm^2)	25
Anode and Cathode Diffusion Layer Thickness (cm)	0.02
Anode and Cathode Catalytic Layer Thickness (cm)	0.0012
Membrane Thickness – Nafion 112 (cm)	0.0051

The main goal of this work is to study the influence of the membrane thickness and transport properties, of the GDL thickness and structure, of the reactants pressure and humidification temperatures on the water content through the membrane and on the cell performance.

3.1 Influence of Membrane Thickness

In order to study the influence of the membrane thickness simulations were performed with four different membrane thicknesses. The polarization curves obtained are shown in Figure 2.

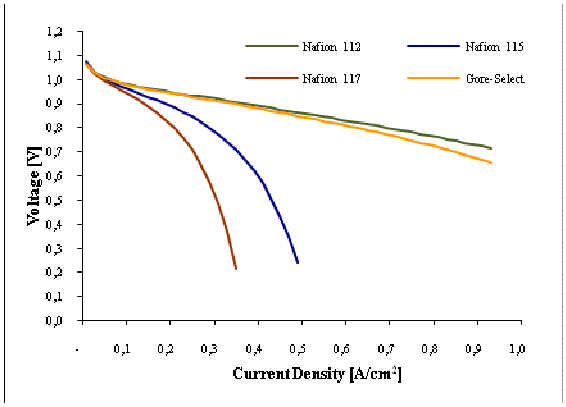

Figure 2 – Voltage vs. Current density for differents membrane thicknesses: Nafion 112 (0.0051 cm), Nafion 115 (0.0127 cm), Nafion 117 (0.0178 cm) and Gore-Select (0.003 cm).

As can be seen in Figure 2, best performances are obtained for Nafion 112 and Gore Select, the thinner membranes. Thicker membranes with higher transfer resistances retain less water and provide lower proton conductivities. It is therefore useful to calculate the water membrane retained at

each membrane. Simulation results for the membrane water content are presented in Figure 3.

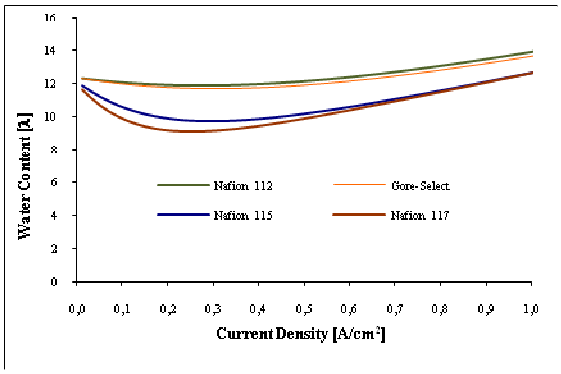

Figure 3 – Menbrane water content vs. Current density for differents membrane thicknesses: Nafion 112 (0.0051 cm), Nafion 115 (0.0127 cm), Nafion 117 (0.0178 cm) and Gore-Select (0.003 cm).

As expected, the membrane water content values are lower for thicker membranes. Thinner membranes with lower mass transfer resistances generate higher water fluxes increasing fuel cell performance. Since the anode and cathode humidification temperatures are the same, back diffusion occurs due to the water production at the cathode. In thinner membranes, the water back diffusion seems to help to counteract the anode drying effect. Concerning the two thinner membranes, although Gore-Select is more thin than Nafion 112, the water diffusivity in Gore-Select membrane is half than in Nafion 112 resulting in a slight lower performance and water content.

3.2 Influence of GDL thickness

To predict the effect of anode and cathode gas diffusion layer thickness, two commercial carbon papers with different thicknesses (SGL Carbon 21-BA, 0.02 cm, SGL Carbon 10-BB, 0.042 cm) were used. The model predictions are shown in Figures 4 and 5.

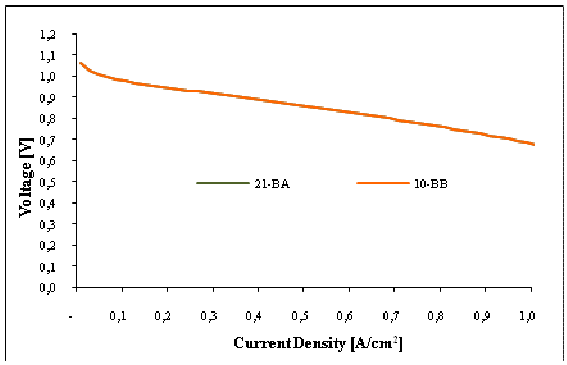

Figure 4 – Voltage vs. Current density for differents anode gas diffusion layers thicknesses: SGL Carbon 21-BA 117 (0.020 cm) and SGL carbon 10-BB (0.042 cm). Membrane Nafion 112.

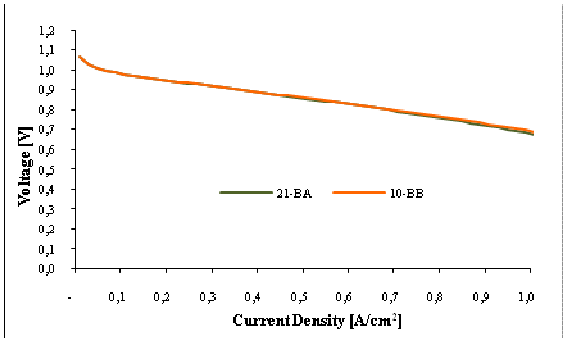

Figure 5 – Voltage vs. Current density for differents cathode gas diffusion layers thicknesses: SGL Carbon 21-BA 117 (0.020 cm) and SGL carbon 10-BB (0.042 cm). Membrane Nafion 112.

As can be seen from Figures 4 and 5, the anode and cathode GDL thickness has for the studied conditions a negligible effect on cell performance. The model predictions for the membrane water transport content, presented in Figures 6 and 7, are in accordance with the results presented in the two previous Figures since the water content is practically insensitive to the variation in the GDL thickness.

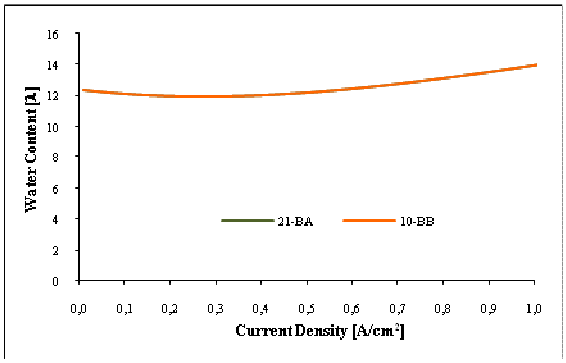

Figure 6 – Menbrane water content vs. Current density for differents anode gas diffusion layers thicknesses: SGL Carbon 21-BA 117 (0.020 cm) and SGL carbon 10-BB (0.042 cm).

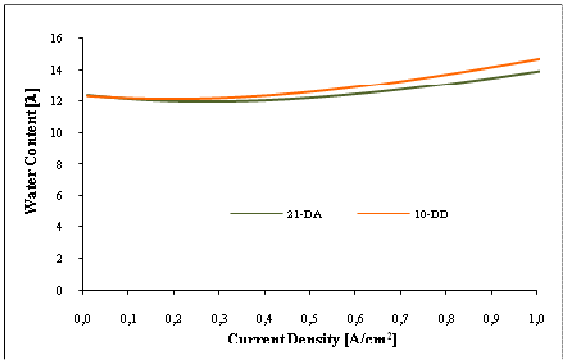

Figure 7 – Menbrane water content vs. Current density for differents cathode gas diffusion layers thicknesses: SGL Carbon 21-BA 117 (0.020 cm) and SGL carbon 10-BB (0.042 cm).

For the studied conditions, particularly for the anode and cathode relative humidity levels, the membrane has a high humidification level and accordingly the impact of the resistance to water transport is not significant. This fact is reinforced by the relatively high effective gaseous diffusion coefficients.

3.3 Influence of reactants pressure

The influence of reactants pressure was studied for both fuel cell sides and for three different inlet pressures. Polarization curves are presented in Figures 8 e 9, while membrane water content results are plotted in Figures 10 e 11.

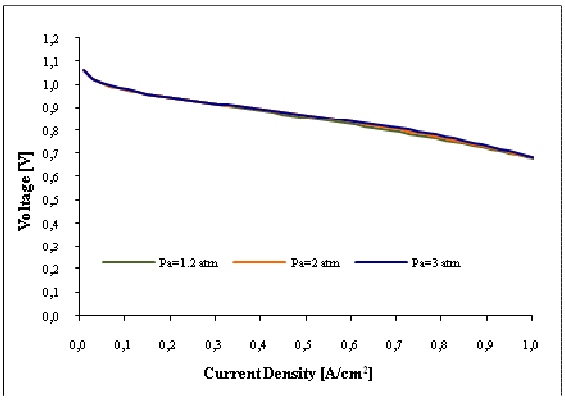

Figure 8 – Voltage vs. Current density for differents anode gas inlet pressures.

As is evident from Figure 8, the influence of the anode inlet pressure is not significant for the anode and cathode relative humidity levels studied

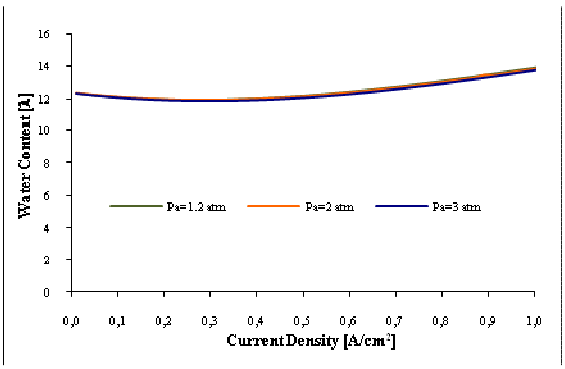

Figure 9 – Menbrane water content vs. Current density differents anode gas inlet pressures.

The water content (Figure 9) is very similar for all the experiments, and, consequently, the polarization curves present almost the same behavior, although a slightly higher result is obtained for higher pressures.

When testing different pressures for the reactants at the cathode the trend is similar. Under the conditions studied, the membrane is well hydrated (Figure 11) with a slight higher water content corresponding to the highest pressure. The higher performances are obtained for the pressurized cathode (4 atm) due to an enhanced oxygen reduction reaction rate resulting from an increase in its partial pressure (Figure 10).

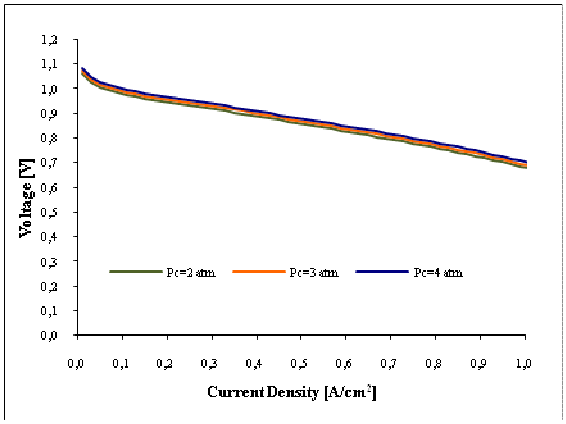

Figure 10 – Voltage vs. Current density for differents cathode gas inlet pressures.

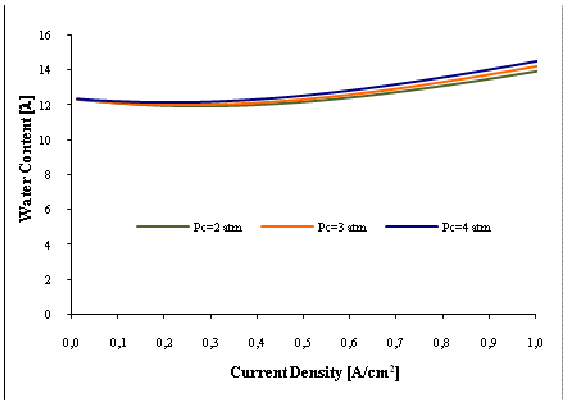

Figure 11 – Menbrane water content vs. Current density for differents cathode gas inlet pressures.

3.4 Influence of humidification temperatures

The influence of reactants humidification temperature was studied for both fuel cell sides and for three different temperatures. Polarization curves are presented in Figures 12 e 13 and membrane water content results in Figures 14 e 15.

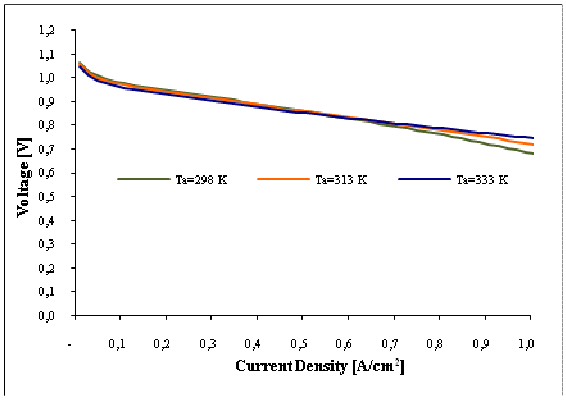

Figure 12 – Voltage vs. Current density for differents anode humidification temperatures.

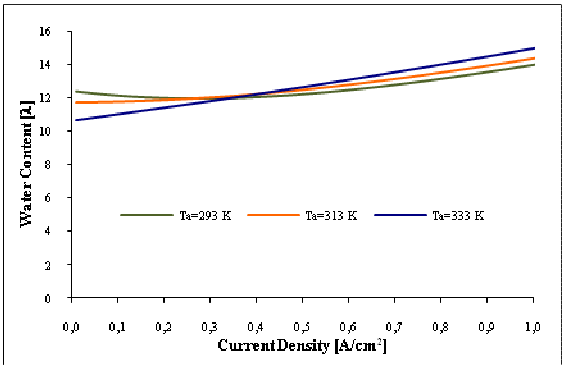

Figure 13 – Menbrane water content vs. Current density for differents anode humidification temperatures.

The water acts like a proton shuttle in the membrane and catalyst layers since excessive water amounts filling the pores inhibit the access to active sites and block the transport of gaseous reactants and products. By the contrary, dehydration of anodic regions due to electro-osmotic drag can cause a breakdown of proton conductivity and even a structural degradation of the PEM.

As can be shown in Figure 12, for lower current densities the fuel cell performance is practically insensitive to the anode humidification temperature. The model results represented in Figure 13 put in evidence that the water content in the membrane is higher for lower humidification temperatures. However, for low current densities, there is no need of high water concentration at the anode since the water transport by electro-osmotic drag is low. For high current densities, better performances are obtained for higher anode humidification temperatures and higher water contents. Under these condition, the electro-osmotic drag is considerable and the water transport by back-diffusion is not enough to prevent membrane dehydration, so more water is required. For high current densities it is therefore useful to work with an increased anode humidification temperature in order to obtain high water concentration at the anode side.

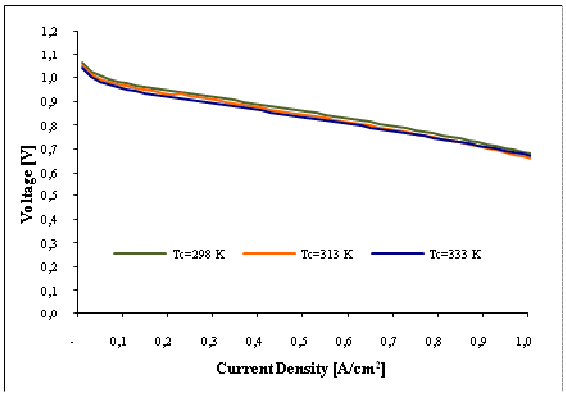

Figure 14 – Voltage vs. Current density for differents cathode humidification temperatures.

At the cathode side, the fuel cell performance is slightly enanched by lower humidification temperatures, as can be seen in Figure 14. These conditions correspond to higher water contents as shown in Figure 15 probably generating an enhanced proton conductivity.

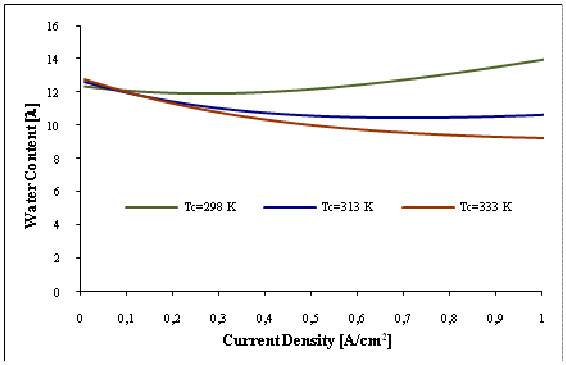

Figure 15 – Menbrane water content vs. Current density for differents cathode humidification temperatures.

4 Conclusions

In the present study, a previous developed model is used to predict the influence of the membrane thickness and transport properties, of the GDL thickness and structure, of the reactants pressure and humidification temperatures on the water content through the membrane and on the cell performance.

For all the conditions studied, a better fuel cell performance corresponds to higher water contents in the membrane.

Cell performance was improved in thinner membranes because the water flux through membrane increases (lower resistance to mass transfer).

The anode GDL thickness has practically no influence in the fuel cell performance while thicker cathode GDLs lead to slightly enhanced fuel cells.

Under the anode and cathode relative humidity levels considered the fuel cell performance is practically insensitive to the pressure of reactants.

For the studied operating conditions, better results are obtained for lower cathode humidification temperatures, which can be a useful information for room temperature applications.

The use of this easy to implement model is practical to achieve optimized tailored MEAS and adequate operating conditions to different applications.

Acknowledgements

The partial support of "Fundação para a Ciência e Tecnologia - Portugal" through project POCI/EME/55497/2004 and scholarship SFRH/BD/28166/2006 is gratefully acknowledged. POCI (FEDER) also supported this work via CEFT

References

[1] D.S. Falcão, V.B. Oliveira, C.M. Rangel, C. Pinho and A.M.F.R. Pinto. Water transport through a PEM fuel cell: A one-dimensional model with heat transfer effects, *Chemical Engineering Science* (2009), doi:10.1016/j.ces.2009.01.049

[2] M. Eikerling; Yu.I. Kharkats; A.A. Kornyshev; Yu.M. Volfkovrch. Phenomenological theory of electro-osmotic effect and water management in polymer electrolyte proton-conducting membranes. *Journal of Electrochemical Society,* Vol. 145 (1998) 2684–2699.

[3] M. Eikerling, A.A. Kornyshev and A.R. Kucerhak. Water in Polymer Electrolyte Fuel Cells: Friend or Foe?. *Physics Today*, Vol.59 (2006), 38-44.

[4] J.J. Baschuk, X. Li. Modeling of polymer electrolyte membrane fuel cells with variable degrees of water flooding. *Journal of Power Sources*, Vol. 86 (2000), 181-195.

[5] Z.H. Wang, C.Y. Wang, K.S. Chen. Two-phase flow and transport in the air cathode of proton exchange membrane fuel cells. *Journal of Power Sources*, Vol. 94 (2001), 40-50.

[6] T.E. Springer, T.A. Zawodzinski, S. Gottesfeld. Polymer-electrolyte fuel cell model. *Journal of Electrochemical Society*, 138 (8) (1991), 2334-2342.

[7] D.M. Bernardi, M.W. Verbrugge. A mathematical model of the solid-polymer-electrolyte fuel cell. *Journal of Electrochemical Society*, 139 (9) (1992), 2477-2491.

[8] A.A. Kulikovsky. Semi-analytical 1D+1D model of a PEMFC. *Electrochemistry Communications*, Vol. 6 (2004), 969–977.

[9] A. Biyikoglu. Review of proton exchange fuel cell models. *International Journal of Hydrogen Energy*, Vol. 30 (2005), 1185-1212.

[10] H. Chang, J.R. Kim, J.H. Cho, H.K. Kim and K.H. Choi. Materials and processes for small fuel cells. *Solid State Ionics*, Vol. 148 (2002), Number 3, 601-606.

[11] R. O' Hayre, S.W. Cha, W. Colella, F.B. Prinz. Fuel Cells Fundamentals. *John Wiley & Sons*, New York, 2006.

[12]X. Ye, C.Y. Wang, (2007). Measurement of Water Transport Through Membrane-Electrode Assemblies I. Membranes. *Journal of Electrochemical Society*, Vol. 154 (7) (2007), B676-B682.